Tuning Mechanism-Based Inactivators of Neuraminidases: Mechanistic and Structural Insights**

Sabrina Buchini, François-Xavier Gallat, Ian R. Greig, Jin-Hyo Kim, Soichi Wakatsuki, Leonard M. G. Chavas,* and Stephen G. Withers*

Abstract: 3-Fluorosialosyl fluorides are inhibitors of sialidases that function by the formation of a long-lived covalent active-site adduct and have potential as therapeutics if made specific for the pathogen sialidase. Surprisingly, human Neu2 and the Trypanosoma cruzi trans-sialidase are inactivated more rapidly by the reagent with an equatorial fluorine at C3 than by its axial epimer, with reactivation following the same pattern. To explore a possible stereoelectronic basis for this, rate constants for spontaneous hydrolysis of the full series of four 3-fluorosialosyl fluorides were measured, and ground-state energies for each computed. The alpha (equatorial) anomeric fluorides hydrolyze more rapidly than their beta anomers, consistent with their higher ground-state energies. However ground-state energies do not explain the relative spontaneous reactivities of the 3-fluoro-epimers. The three-dimensional structures of the two 3-fluoro-sialosyl enzyme intermediates of human Neu2 were solved, revealing key stabilizing interactions between Arg21 and the equatorial, but not the axial, fluorine. Because of changes in geometry these interactions will increase at the transition state, likely explaining the difference in reaction rates.

Sialic acid is found as the terminal sugar on many mammalian cell surface glycans, where it plays an important role in mediating interactions of cells with their environment.[1] These interactions may be involved in normal cell functions or may occur when a cell is attacked by pathogens bearing sialic acid-binding proteins on their surfaces. Some parasites such as *Trypanosoma cruzi* are incapable of biosynthesizing sialic acid, and require the expression of a cell surface *trans*-sialidase to scavenge sialic acids from host glycans and thereby decorate their own surfaces as part of the infection process.[2] Bacteria such as *Hemophilus influenzae*, *Streptococcus pneumoniae*, and *Pseudomonas aeruginosa* also produce neuraminidases that are thought to remove sialic

acid from epithelial cell surfaces, exposing bacterial receptors, though the roles of these neuraminidases in the pathogenesis of infection are not well understood. The influenza virus likewise carries a surface neuraminidase to liberate itself from cell surface confinement after budding. Neuraminidase inhibitors have therefore attracted attention, not only as antivirals (Relenza and Tamiflu for treatment of flu) but also as potential antimicrobials.[3] Humans also produce neuraminidases: *h*Neu1 (intra lysosomal), *h*Neu2 (cytosolic), *h*Neu3 (plasma membrane), and *h*Neu4 (lysosomal or mitochondrial membrane). The four enzymes all belong to the same sequence-related family (GH33 in the CAZy classification) as their bacterial and trypanosomal counterparts, though distinct from that (GH34) of the viral enzymes. Consequently any inhibitor design must incorporate specificity-determining elements to avoid unwanted effects on the host.

Our laboratory has introduced 3-fluorosialosyl fluorides (difluorosialic acids, DFSAs) as a class of mechanism-based neuraminidase inhibitors that function by forming transient covalent adducts, and has had some success in developing analogs with improved specificity for pathogen neuraminidases over their human counterparts, with the recent work on influenza neuraminidase inhibitors being particularly relevant.[4] Three-dimensional structures of the trapped 3-fluorosialyl enzyme intermediates of the influenza virus enzyme and of the *T. cruzi trans*-sialidase (*Tc*TS) have been published, but not that of a complex with a human neuraminidase.[4,5] To optimize specificity, such structural insights are needed, as they will provide a better understanding of the active-site environment of the human enzyme and of the consequences on reaction rates of changing stereochemistry at the site of fluorine substitution (C3). Here we report the first three-dimensional structures of covalent sialyl-enzyme intermediates formed with a human neuraminidase using both 3-fluoro (equatorial) and 3-fluoro (axial) sialic acid reagents. We also explore the consequences of modifying the stereochemistry at C3 on enzyme inactivation and reactivation behaviors with two different GH33 sialidases, as well as underlying effects on the nonenzymatic solvolysis, coupled to computational analysis.

Sialidases and *trans*-sialidases from the GH33 family employ a two-step double displacement mechanism in which an active-site tyrosine functions as a nucleophile and reaction proceeds through oxocarbenium ion-like transition states.[6] The 3-fluorosialyl fluorides function as mechanism-based inactivators by forming a long-lived sialyl-enzyme intermediate (Figure 1). The fluorine at C3 destabilizes the oxocarbenium ion-like transition states, slowing both steps in the mechanism, while the equatorial anomeric fluoride at C2

[*] Dr. S. Buchini, Dr. I. R. Greig, Dr. J.-H. Kim, Prof. Dr. S. G. Withers
Department of Chemistry, University of British Columbia
Vancouver, B. C., V6T 1Z1 (Canada)
E-mail: withers@chem.ubc.ca

F.-X. Gallat, Prof. S. Wakatsuki, Prof. Dr. L. M. G. Chavas
Structural Biology Research Center
Photon Factory Institute of Materials Structure Science
High Energy Accelerator Research Organization (KEK)
Tsukuba, Ibaraki 305-0801 (Japan)
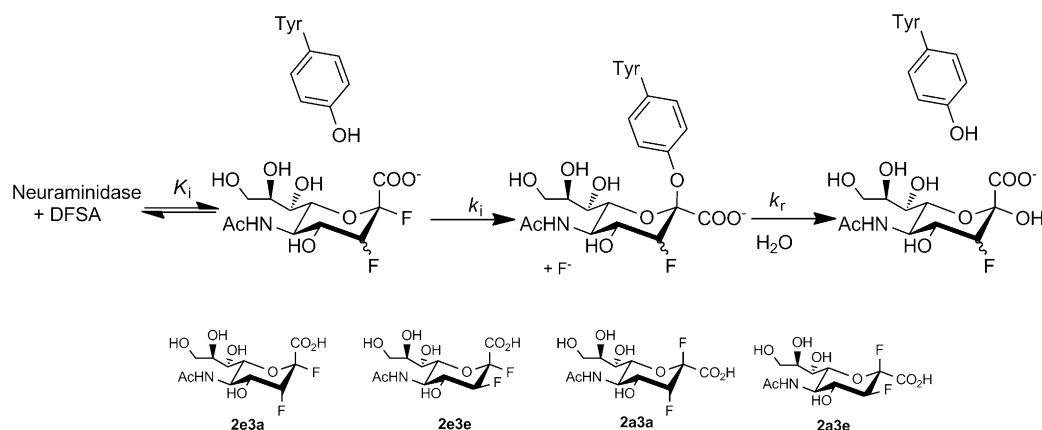E-mail: leonard.chavas@kek.jp

Figure 1. Mechanism of neuraminidase inactivation by 2,3-difluorosialyl fluorides and structures of difluorosialic acids studied. Slowing of the de-sialylation step (k_r) by inductive destabilization of the oxocarbenium-ion-like transition state leads to accumulation of the covalent intermediate, thus inactivation.

also obtained by fluorination of protected DANA (2-deoxy-2,3-didehydro-*N*-acetyl-neuraminic acid) using xenon difluoride. This yielded the axial anomeric fluoride derivative directly and the equatorial derivative by aqueous acid hydrolysis of the axial anomeric fluoride followed by re-protection and the treatment described above (see Scheme S2).

serves as a good leaving group, making the intermediate accessible.[7] All inactivation studies of GH33 enzymes to date with this DFSA class of inhibitor have employed the derivative with an axial fluorine at C3. However, our recent studies with the GH34 influenza neuraminidase revealed significant differences in rates of inactivation and reactivation for sialic acids with axial versus equatorial fluorines at C3. Likewise, a single earlier report had shown that GT80 sialyltransferases process the corresponding equatorial CMP-3-fluorosialic acid derivative faster than the axial analog,[8] piquing our interest in how the two C3 epimers are processed by human sialidases and by *Tc*TS, and what underlies this behavior. We chose *h*Neu2 as the representative human sialidase since it is the only such mammalian enzyme for which structural information is available.[9] Further, in order to better understand the effects of the two fluorine substitutions on the inherent reactivity of sialosides we synthesized the full set of DFSAs (listed in Figure 1), measured rates of nonenzymatic hydrolysis for each, and performed quantum calculations of ground-state energies.

Synthesis of 3-fluorosialic acid for conversion into its two anomeric fluorides was achieved by incubation of 3-fluoropyruvic acid with *N*-acetylmannosamine in the presence of the *E. coli* Neu5Ac aldolase, yielding a mixture of the two 3-fluoro epimers, as described previously.[8,10] After protection of the acid and alcohols as esters the two compounds were separated by silica gel chromatography and subjected to anomeric deprotection with hydrazine acetate. Reaction of these hemiketals, individually, with DAST (diethylaminosulfur trifluoride) yielded mixtures of the two anomeric fluorides, which were separated by column chromatography and then deprotected (see Scheme S1 in the Supporting Information). The 3-fluoro (equatorial) sialic acid derivatives were

Kinetic analysis of the interaction of **2e3e** with *Tc*TS revealed rapid inactivation (Table 1). Indeed measurements at concentrations above 0.5 mM could not be made because inactivation was too fast, thwarting attempts to observe saturation behavior. Nonethe-

Table 1: Kinetic parameters for inactivation and reactivation of *Tc*TS and human Neu2 by 3ax- and 3eq-difluorosialic acids.

Inhibitor	*Tc*TS k_i/K_d [×10^{-3} min^{-1} mM^{-1}]	*Tc*TS k_r [×10^{-3} min^{-1}]	Neu2 k_i/K_d [×10^{-3} min^{-1} mM^{-1}]	Neu2 K_i (app) [μM][b]
2e3a	8.0 ± 0.4	≈ 0[a]	1440 ± 72	ND
2e3e	471 ± 76	17.4 ± 1.6	ND	28

ND = Not Detected. [a] Reactivation occurs only in the presence of sugar acceptor (e.g. Lactose). [b] Determined from analysis of the Dixon plot.
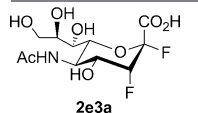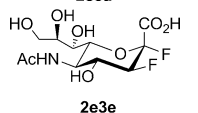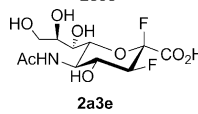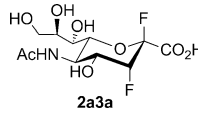
less a second-order rate constant of 471×10^{-3} min^{-1} mM^{-1} was measured from the slope of the plot of the inactivation rate versus the **2e3e** concentration. This is approximately 60-fold faster than the inactivation caused by the axial epimer **2e3a**.[10a] To assess turnover (reactivation) rates, a sample of *Tc*TS inactivated by **2e3e** was freed of excess inactivator by gel filtration, incubated in buffer at 25 °C, and samples removed and assayed at time intervals. Fitting of the data to a simple first-order expression revealed a reactivation rate constant of 1.7×10^{-2} min^{-1}, corresponding to a half-life of approximately 40 minutes (see Figures S2 and S3). The formation of 3-fluorosialic acid as shown by mass spectrometry confirmed the hydrolytic turnover nature of the reactivation (Figure S6). By comparison, no significant hydrolytic reactivation of the enzyme trapped by the axial epimer was observed.[10] Taken together, these data show that an equatorial fluorine at C3 clearly has a less rate-retarding effect on both steps of the enzymatic reaction than does an axial fluorine.

A similar trend, though manifested somewhat differently, was seen for *h*Neu2. In this case the axial anomer **2e3a** inactivated the enzyme according to a second-order rate constant of $k_i/K_d = 1.44 \ \text{min}^{-1} \text{mM}^{-1}$ while reactivation occurred with $k_{hyd} = 6 \times 10^{-4} \ \text{min}^{-1}$, corresponding to a half-life of approximately 20 h (see Figure S4). By contrast, no time-dependent inactivation was observed with the equatorial epimer **2e3e**, which instead functioned as a slow substrate, but one for which the deglycosylation step (k_{hyd}) is slower than the inactivation step (k_i). This kinetic behavior is revealed in the surprisingly tight apparent binding of **2e3e** when tested as a competitive inhibitor ($K_{iapp} = 28 \ \mu\text{M}$), which arises because most of the enzyme accumulates as its fluorosialyl-enzyme species (Figure S5). This is a much higher "affinity" than would be anticipated based upon its simple structure, thus suggesting that, as with *Tc*TS, both formation and hydrolysis of the 3-fluorosialyl-*h*Neu2 intermediate are much faster with the equatorial 3-epimer than the axial and that the intermediate is accumulating under assay conditions.

To gain some insight into the source of this fascinating difference in reactivity of the 3-fluoro equatorial and axial derivatives, we investigated the spontaneous hydrolysis of the full series of the four DFSAs (**2e3e**, **2e3a**, **2a3a**, **2a3e**; Figure 1) to establish whether this difference arose from inherent stereoelectronic effects, or was primarily a consequence of enzymatic interactions. Hydrolysis rates were determined by incubating samples in 50 mм buffer containing 1м NaClO₄ in sealed vials, removing aliquots at time intervals and freezing them immediately. At the end of the time-course, samples were thawed and their fluoride concentrations measured using a fluoride-selective electrode. The pH dependence of hydrolysis was first probed for **2e3a** and **2e3e** at a series of pH values, and reaction rates shown to be pH-independent between pH 5 and 8 (Figure S7), as previously reported for the hydrolysis of aryl sialosides.[11] To ensure which ionic forms are present under these conditions, $\text{p}K_a$ values for the carboxylic acids of each DFSA were measured by back-titration of their acid forms using sodium hydroxide and found to lie between 2.3 and 2.4 (Table 2; Table S1 and Figure S9). Such values are lower than those of 2.8 and 2.6 measured for the parent sialic acid and its methyl glycoside, respectively, consistent with the presence of a second fluorine in the DFSAs. Further, the near identity of these four DFSA $\text{p}K_a$ values shows that the different stereochemistries of the fluorines play no role. The pH independence of the hydrolysis rates and the near identical $\text{p}K_a$ values therefore confirm that the reaction of the deprotonated (monoanionic) substrate under these conditions occurs by spontaneous heterolysis of the C−F bond. With this established, first-order rate constants for hydrolysis of the four DFSA substrates (**2e3e**, **2e3a**, **2a3e**, **2a3a**) were measured at pH 7 (Table 2; Figures S7 and S8).

The first and most striking observation is that the α-sialyl fluorides (equatorial leaving group) hydrolyze much faster than the β anomers: 36-fold faster in the 3-fluoro (ax) pair and 631-fold faster in the 3-fluoro (eq) pair. This reactivity difference is reminiscent of the 40-fold rate difference reported between α- and β-glucosyl fluoride solvolyses and attributed to differences in ground-state stabilities that are minimized at the (highly dissociative) transition state.[12] To

Table 2: $\text{p}K_a$ values, rate constants for spontaneous hydrolysis and computed relative ground state energies for difluorosialic acids.

Inhibitor	$\text{p}K_a$	k_{hyd} [×10⁻⁶ min⁻¹]	Relative ground-state energy [kJ mol⁻¹]
2e3a	2.3	100	0
2e3e	2.4	820	−1.4
2a3e	2.3	1.3	−6.6
2a3a	2.3	2.8	−9.0

gain deeper insight into these relative ground-state stabilities we computed the energy differences between the ground states of the four DFSAs. Indeed, the sialosyl fluorides possessing axial anomeric fluorides were found to be more stable than those possessing equatorial anomeric fluorides as predicted by the anomeric effect, with **2a3a** being 2.4 kJ mol⁻¹ more stable than **2a3e**, and **2e3e** 1.4 kJ mol⁻¹ more stable than **2e3a** (Table 2; Figure S10). This pattern of stabilities of the 3-epimeric pairs of compounds is consistent with expected stabilities arising from the interaction of carbon–heteroatom bond dipoles between C2 and C3 centers. For example, while **2a3a** possesses a stabilizing antiparallel orientation between C3−F and C2−F bond dipoles, the antiparallel orientation of **2a3e** only exists between C3−F and C2−O6 bond dipoles, with the C2−O7 bond dipole expected to be smaller. Similarly, **2e3e** shows an antiparallel orientation between C3−F and C2−O6 bond dipoles, but **2e3a** has no antiparallel orientations between C2-heteroatom and C3-heteroatom dipoles. These relative ground state stabilities are therefore consistent with the relative rates observed for compounds with axial and equatorial leaving groups. The present conclusions also concur with previously reported results in which mono-anions of aryl α-sialosides were found to hydrolyse 100-fold faster than their β counterparts.[11b] In this earlier report, the difference was largely attributed to the release of steric strain arising from the axial carboxy group in the ground state of the α-sialosides, though undoubtedly the effects seen in that case were moderated by the counteracting release of steric strain arising from departure of the bulky aryl leaving group. That counteracting steric effect would not be significant in the present case, with sterically modest fluoride leaving groups.

The computed relative ground-state stabilities do not, however, reflect the measured rate differences between C-3 epimers possessing leaving groups of the same geometry since, for example, **2a3a** is found to have a lower energy than **2a3e**, yet is hydrolyzed two-times faster (corresponding to a transition state theory (TST)-predicted activation energy difference of 2.1 kJ mol⁻¹; Table 2). Likewise, **2e3e** is found to

have a lower energy than **2e3a**, yet is hydrolyzed eight-times faster (TST activation energy difference of 5.7 kJ mol^{-1}). Clearly other factors are more important in determining transition-state stabilities. One possibility, consistent with earlier proposals, is that interactions between electronegative pyranose ring substituents and the water nucleophile may be important in determining rates of pyranosyl fluoride hydrolysis.[12b] In this instance, 3-fluoro substituents disposed in an *anti*-fashion to the leaving group anomeric fluoride may enhance the nucleophilicity of the incoming water molecules through a hydrogen-bonding interaction. Similar effects were seen in the hydrolysis of 2,4-dinitrophenyl β-glycosides and their 2-deoxy-2-fluoro analogs, where substrates with an axial C-2 substituent (manno- and 2-fluoromanno) hydrolyzed five times slower than their 2-epimers.[13]

Whatever the sources of these differences, the effects are relatively small compared to those seen with the enzyme, though indeed in the same sense. To gain deeper insight into the nature of the differences in the interactions of the compounds with active-site residues, we determined the three-dimensional structures of *h*Neu2 trapped in the form of the two 3-fluorosialyl-enzyme intermediates, both with the axial and equatorial fluorine (Table S2). The two epimers sit inside the active site of *h*Neu2 in an essentially identical manner, covalently bound to the human enzyme by Tyr334 and stabilized by an extended hydrogen-bond network involving nine residues and two structured water molecules (Figure 2). While the axial epimer orients its fluorine to the solvent, the equatorial fluorine makes contacts (2.6 and 3.1 Angstroms) with the two terminal nitrogen atoms (N1 and N2 respectively) of Arg21. This arginine also interacts closely with the substrate C1 carboxylate. Interactions between fluorine and protonated nitrogen are well-documented and have been computed at up to 13.5 kcal mol^{-1}.[14] Therefore, especially if optimized at the transition state as they are likely to be due to the conformational changes occurring, these interactions could readily explain the difference in rates between the equatorial and axial derivatives. Interestingly similar interactions are seen in the influenza neuraminidase between the equatorial fluorine of the covalently bound DFSA and Arg118 in that case.[4]

While the large differences in rates of spontaneous hydrolysis of DFSAs of opposite anomeric stereochemistry are due largely to differences in ground-state stability, the more subtle differences in rate constants for the 3-epimeric DFSA pairs arise instead largely from differences in the transition-state structure. Likewise the very different rate constants for inactivation and reactivation of *Tc*TS and Neu2 by these 3-epimeric DFSAs arise primarily from differential transition-state stabilization. Three-dimensional structures of the two 3-fluorosialyl-enzyme intermediates of human Neu2 suggest that interactions between the equatorial fluorine and the highly conserved Arg21 could play particularly important roles in binding of the transition states for the two steps and are responsible for the large rate differences observed. These factors should be considered in any future design of inhibitors of this class for other neuraminidases.
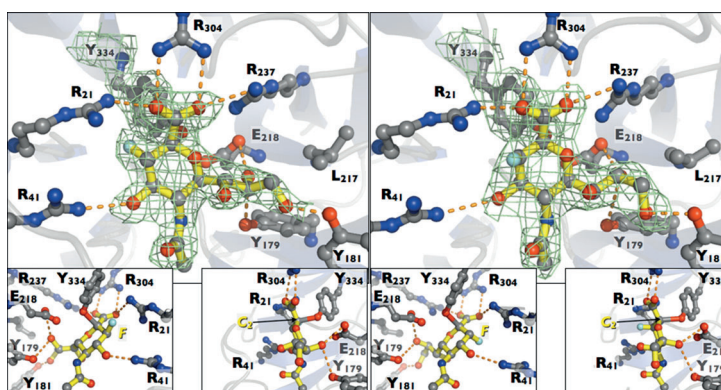

Figure 2. X-ray structures of the covalent intermediates trapped on Neu2 with 3F-equatorial and 3F-axial substituents. Left panels: structure with 3F-equatorial sialic acid. Right panels: structure with 3F-axial sialic acid. Insets show alternative views.

Experimental Section

Details of all synthetic steps and product characterization are provided in the Supporting Information, as are full details of enzymatic and spontaneous kinetic analyses, computational methods, and X-ray structure determination. Optimized geometries and frequencies were determined at the IEF-PCM/M06-2X/6-31 + G-(d,p) level of theory. Energies for these optimized geometries were recalculated at the SMD/M06-2X/6-31 + G(d,p) level of theory. These methods have previously proved reasonably accurate in the investigation of the reaction energetics of a series of fluoroxylosides.[12b]

[1] A. Varki, *Trends Mol. Med.* **2008**, *14*, 351.

[2] A. C. C. Frasch, *Parasitol. Today* **2000**, *16*, 282.

[3] a) G.-Y. Chen, X. Chen, S. King, K. A. Cavassani, J. Cheng, X. Zheng, H. Cao, H. Yu, J. Qu, D. Fang, W. Wu, X.-F. Bai, J.-Q. Liu, S. A. Woodiga, C. Chen, L. Sun, C. M. Hogaboam, S. L. Kunkel, P. Zheng, Y. Liu, *Nat. Biotechnol.* **2011**, *29*, 428; b) M. von Itzstein, *Nat. Rev. Drug Discovery* **2007**, *6*, 967; c) M. von Itzstein, W. Y. Wu, G. B. Kok, M. S. Pegg, J. C. Dyason, B. Jin, T. Van Phan, M. L. Smythe, H. F. White, S. W. Oliver, P. M. Colman, J. N. Varghese, D. M. Ryan, J. M. Woods, R. C. Bethell, V. J. Hotham, J. M. Cameron, C. R. Penn, *Nature* **1993**, *363*, 418.

[4] J. H. Kim, R. Resende, T. Wennekes, H. M. Chen, N. Bance, S. Buchini, A. G. Watts, P. Pilling, V. A. Streltsov, M. Petric, R. Liggins, S. Barrett, J. L. McKimm-Breschkin, M. Niikura, S. G. Withers, *Science* **2013**, *340*, 71; C. J. Vavricka, Y. Liu, H. Kiyota, N. Sriwilaijaroen, J. Qi, K. Tanaka, Y. Wu, Q. Li, Y. Li, J. Yan, Y. Suzuki, G. F. Gao, *Nat. Commun.* **2013**, *4*, 1491.

[5] M. F. Amaya, A. G. Watts, I. Damager, A. Wehenkel, T. Nguyen, A. Buschiazzo, G. Paris, A. C. Frasch, S. G. Withers, P. M. Alzari, *Structure* **2004**, *12*, 775.

[6] D. L. Zechel, S. G. Withers, *Acc. Chem. Res.* **2000**, *33*, 11.

[7] a) I. Damager, S. Buchini, M. F. Amaya, A. Buschiazzo, P. Alzari, A. C. Frasch, A. Watts, S. G. Withers, *Biochemistry* **2008**, *47*, 3507; b) A. G. Watts, I. Damager, M. L. Amaya, A. Buschiazzo, P. Alzari, A. C. Frasch, S. G. Withers, *J. Am. Chem. Soc.* **2003**, *125*, 7532.

[8] H. A. Chokhawala, H. Z. Cao, H. Yu, X. Chen, *J. Am. Chem. Soc.* **2007**, *129*, 10630.

[9] a) L. M. Chavas, R. Kato, N. Suzuki, M. von Itzstein, M. C. Mann, R. J. Thomson, J. C. Dyason, J. McKimm-Breschkin, P. Fusi, C. Tringali, B. Venerando, G. Tettamanti, E. Monti, S. Wakatsuki, *J. Med. Chem.* **2010**, *53*, 2998; b) L. M. G. Chavas, C. Tringali, P. Fusi, B. Venerando, G. Tettamanti, R. Kato, E. Monti, S. Wakatsuki, *J. Biol. Chem.* **2005**, *280*, 469.

[10] a) S. Buchini, A. Buschiazzo, S. G. Withers, *Angew. Chem.* **2008**, *120*, 2740; *Angew. Chem. Int. Ed.* **2008**, *47*, 2700; b) A. G. Watts, S. G. Withers, *Can. J. Chem.* **2004**, *82*, 1581.

[11] a) M. Ashwell, X. M. Guo, M. L. Sinnott, *J. Am. Chem. Soc.* **1992**, *114*, 10158; b) V. Dookhun, A. J. Bennet, *J. Am. Chem. Soc.* **2005**, *127*, 7458.

[12] a) A. Konstantinidis, M. L. Sinnott, *Biochem. J.* **1991**, *279*, 587; b) S. S. Lee, I. R. Greig, D. J. Vocadlo, J. D. McCarter, B. O. Patrick, S. G. Withers, *J. Am. Chem. Soc.* **2011**, *133*, 15826.

[13] M. N. Namchuk, J. D. McCarter, A. Becalski, T. Andrews, S. G. Withers, *J. Am. Chem. Soc.* **2000**, *122*, 1270.

[14] L. Shimoni, J. P. Glusker, C. W. Bock, *J. Phys. Chem.* **1995**, *99*, 1194.